Atmos. Chem. Phys. Discuss., 6, 4995–5038, 2006
www.atmos-chem-phys-discuss.net/6/4995/2006/

Atmospheric Chemistry and Physics Discussions

Centennial evolution of the atmospheric methane budget: what do the carbon isotopes tell us?

K. R. Lassey[1], D. M. Etheridge[2], D. C. Lowe[1], A. M. Smith[3], and D. F. Ferretti[1,4]

[1]National Institute of Water and Atmospheric Research, P.O. Box 14-901, Wellington, New Zealand
[2]CSIRO Marine and Atmospheric Research, PMB 1, Aspendale Vic. 3195, Australia
[3]Australian Nuclear Science and Technology Organisation, PMB 1, Menai NSW 2234, Australia
[4]Institute of Arctic and Alpine Research, University of Colorado, Boulder, CO 80309, USA

Received: 6 April 2006 – Accepted: 5 May 2006 – Published: 21 June 2006

Correspondence to: K. R. Lassey (k.lassey@niwa.co.nz)

Abstract

Little is known about how the methane source inventory and sinks have evolved over recent centuries. New and detailed records of methane mixing ratio and isotopic composition ($^{12}CH_4$, $^{13}CH_4$ and $^{14}CH_4$) from analyses of air trapped in polar ice and firn can enhance this knowledge. We use existing bottom-up constructions of the source history, including "EDGAR"-based constructions, to assemble a model of the evolving global budget for methane and for its carbon isotope composition through the 20th century. By matching such budgets to atmospheric data, we examine the constraints imposed by isotope information on those budget evolutions. Balancing both $^{12}CH_4$ and $^{13}CH_4$ budgets requires participation by a highly-fractionating atmospheric sink such as active chlorine (removing at least 10 Tg yr^{-1}), which has been proposed independently. Examining a companion budget evolution for $^{14}CH_4$ exposes uncertainties in inferring the fossil-methane source from atmospheric $^{14}CH_4$ data. Specifically, methane evolution during the nuclear era is sensitive to the cycling dynamics of "bomb ^{14}C" (originating from atmospheric weapons tests) through the biosphere. In addition, since ca 1970, direct production and release of $^{14}CH_4$ from nuclear-power facilities is influential but poorly quantified. Atmospheric $^{14}CH_4$ determinations in the nuclear era have the potential to better characterize biospheric carbon cycling and to better quantify the ill-determined nuclear-power source.

1 Introduction

Despite considerable activity in atmospheric methane research over the past 15–20 years, little is known about how its sources and its sinks have evolved during the agro-industrial era (the past 3 centuries) of profound human influence. This era has seen a 2.5-fold growth in the atmospheric methane burden that has not been fully interpreted in terms of the evolution of methane sources and sinks. The principal cause of this growth is the expansion of agricultural and industrial activities, including livestock farming,

ACPD

6, 4995–5038, 2006

rice cultivation, mining of fossil fuels, reticulation of natural gas, and the large-scale burning of forest and savanna biomass. The detailed histories of these anthropogenic sources is poorly known, notwithstanding efforts to quantify them based on historical activity data (e.g., van Aardenne et al., 2001). Other approaches apply inverse tracer modelling to atmospheric data over limited time ranges (Hein et al., 1997; Houweling et al., 1999; Cunnold et al., 2002; Wang et al., 2004) or global modelling over longer time scales (Etheridge et al., 1998; Lassey et al., 2000) with the latter requiring that the methane sink history be simulated or postulated.

The methane source mix and its evolution can be constrained by isotope data (Fung et al., 1991; Hein et al., 1997; Mikaloff Fletcher et al., 2004). This is because of the distinctive isotopic "signatures" $\delta^{13}C$ and/or $\Delta^{14}C$ (defined in Sect. 2) of different source categories. Specifically, biogenic methane is relatively depleted in the stable isotope ^{13}C ($\delta^{13}C \approx -60‰$), pyrogenic methane (a by-product of biomass combustion) is relatively enriched ($\delta^{13}C > -25‰$), and fossil methane sources are intermediate between these ($\delta^{13}C \approx -40‰$). Furthermore, fossil sources are devoid of the radioisotope ^{14}C, while biogenic and pyrogenic methane sources contain ^{14}C levels characteristic of the atmospheric CO_2 from which the carbon was photosynthetically derived, adjusted for post-photosynthesis decay. The ^{14}C-free property of fossil methane has led investigators to infer the "fossil fraction" of the prevailing methane source from atmospheric $^{14}CH_4$ measurements (Lowe et al., 1988; Wahlen et al., 1989; Manning et al., 1990; Quay et al., 1991, 1999).

Studies of the evolution of atmospheric methane based on measurements of ice-entrapped air started in the early 1970s (Robbins et al., 1973). While corresponding $\delta^{13}C$ determinations were reported from the late 1980s (Craig et al., 1988), sample-size limitations and an unawareness of isotopic fractionation that result from diffusion and from gravitational settling within the entrapped air bubbles precluded detailed and precise time series. Consequently, the budget evolution over long time scales has been poorly constrained. However, longer time series for $^{13}CH_4$ are now available due to small-sample developments that combine gas chromatography and stable isotope

ACPD
6, 4995–5038, 2006

EGU

ratio mass spectrometry (GC-IRMS) (Miller et al., 2002) in conjunction with new techniques for extracting samples of old air trapped in polar firn and ice (Ferretti et al., 2005; Sowers et al., 2005). In particular, such samples from Law Dome, Antarctica, offer highly time-resolved measurements (Trudinger et al., 2002; Ferretti et al., 2005). Parallel developments in accelerator mass spectrometry (AMS) are enabling coarse-resolution air samples to be analyzed for $^{14}CH_4$ (Etheridge et al., 2001).

The methane budget evolution is also impacted by changes to atmospheric sinks. The principal sink (~85%) is in situ oxidation by the OH radical, generated photolytically at a rate that depends in part upon the local presence of pollutants such as hydrocarbons and other volatile organic compounds, CO and NO_x. Minor sinks include consumption by methanotrophic biota in aerated soils, transport to and destruction in the stratosphere, and other atmospheric oxidants such as active chlorine (Allan et al., 2001). Quantitative assessment of the global OH trend is difficult over any time scale. However, various modelling studies agree qualitatively that global OH levels have declined over the industrial era (Lelieveld et al., 1998; Wang and Jacob, 1998; Houweling et al., 2000), but that during recent decades that decline may have been arrested (Lelieveld et al., 2002) or, within decadal intervals, even reversed (Karlsdóttir and Isaksen, 2000; Dentener et al., 2003; Wang et al., 2004). Using measurements of quite different tracers of OH, CH_3CCl_3 (methyl chloroform) and ^{14}CO, Prinn et al. (2005) and Manning et al. (2005) both conclude that global-mean OH has been remarkably stable over the past ~25 years, punctuated only by fluctuations lasting up to a few years that reflect wide-scale perturbations (e.g. eruption of Mt Pinatubo in 1991).

In this paper, we present detailed model analysis of the methane budget evolution over the 20th century during which the atmospheric burden doubled. In investigating the value of carbon-isotope information obtained from both contemporary records and from air trapped in polar ice and firn, we: (a) explore the constraints imposed on the reconstruction by high-resolution $^{13}CH_4$ measurements, and (b) assess the information conveyed by $^{14}CH_4$ ("radiomethane") measurements.

2 Modelling strategy

Global methane mass balance requires that:

$$\frac{\partial C(t)}{\partial t} = S(t) - \lambda(t)C(t) \quad (1)$$

where $S(t)$, $\lambda(t)$ and $C(t)$ are the global source (Tg yr^{-1}), sink (yr^{-1}) and tropospheric burden (Tg) respectively of methane at time t. The same equation applies separately to each "methane isotope", $^{12}CH_4$, $^{13}CH_4$ and $^{14}CH_4$, but with $\lambda(t)$ augmented by radioactive decay, λ_R, in the case of $^{14}CH_4$. The tropospheric burden is taken to be directly proportional to mean surface mixing ratio at 2.767 Tg ppb^{-1} (Fung et al., 1991; Dlugokencky et al., 1998). Mixing ratios cited in this paper are expressed on the CMDL83 scale. Adoption of the newer NOAA04 scale (Dlugokencky et al., 2005) would adjust mixing ratios by 1.24% with an indiscernible impact on budgeting.

A corollary of Eq. (1) is that the specification of any two of $S(t)$, $\lambda(t)$ and $C(t)$ over a time duration enables the third to be inferred through "budget closure". Of these, $C(t)$ is the best-determined through the history of methane mixing ratio. Etheridge et al. (1998) have constructed such a history, 1000–1992, based on analyses of air extracted from Antarctic firn and ice cores, and of air archived since 1978 at Cape Grim Observatory (CGO), Australia (Francey et al., 1999). This time series blends with contemporary measurements since 1984 based on the NOAA/CMDL monitoring network (Dlugokencky et al., 1998, 2003). Thus with $C(t)$ specified, budget closure can be achieved by either: (a) prescribing the methane sink history and inferring a corresponding source history; or (b) constructing the source history and inferring a corresponding sink history. The former option is commonly pursued using a time-invariant sink (Dlugokencky et al., 1998; Lassey et al., 2000), while the present work applies the latter option for total methane then the former option for individual isotopes.

The methane mixing ratio appears to have been fairly stable at ~693 ppb near ca 1700 AD (Etheridge et al., 1998, Fig. 2) after which it rose almost monotonically. This

ACPD
6, 4995–5038, 2006

EGU

suggests that the methane cycle would be close to steady state in ca 1700, even if suppressed during the cooler temperatures of the "Little Ice Age", ca 1300 AD–1850 AD (Etheridge et al., 1998). We therefore commence our model integration at an imposed steady state in 1700, as per Lassey et al. (2000), using annual time steps through to the most recent year specified by the source history. The annualized time series $C(t)$ merges the Etheridge et al. (1998) record from 1700, interpolated where necessary, with the NOAA/CMDL composite dataset (E. J. Dlugokencky, personal communication, 2004). The merged record is referred to as the Etheridge-extended dataset.

Each source construction is likewise specified as an annual time series from 1700 (Sect. 3), even if extrapolation back to 1700 has little supporting data. Commencing integration as early as 1700 enables the history of post-1700 disequilibrium in both mixing ratio and δ^{13}C to be plausibly simulated (Lassey et al., 2000), having regard to the slow response of atmospheric δ^{13}C to source perturbations (Tans, 1997).

Integration over 1-year time steps perforce ignores seasonality. This is unavoidable, not only because source constructions lack seasonal information, but also because the air enclosure process in the Law Dome firn and ice smoothes out compositional variations over five years or more (Trudinger et al., 2002). However, the neglect of seasonality is also reasonable when examining changes over centennial timescales. Within each time step the source and sink are held constant, enabling analytic integration of Eq. (1) so that the burden propagates from C_{beg} to C_{end} during a time step of duration Δt, given by:

$$C_{\mathrm{end}} = S/\lambda + \left(C_{\mathrm{beg}} - S/\lambda\right)\ \exp(-\lambda \Delta t) \qquad (2)$$

We apply three alternative constructions of the source history (Sect. 3), annualizing as necessary and plausibly extrapolating back to 1700. With the atmospheric burden $C(t)$ and source history $S(t)$ both specified at annual time steps from 1700, the mass-balancing sink history $\lambda(t)$ is deduced by solving Eq. (2) numerically for λ within each time step (Sect. 3). This sink history, adjusted for time-independent isotope fractionation, is then applied separately to $^{12}CH_4$ and $^{13}CH_4$ budgets, and budget closure

ACPD
6, 4995–5038, 2006

addressed through both forward and inverse modelling (Sect. 4). For the $^{14}CH_4$ budget, both source and sink histories are constructed and the resulting atmospheric history examined (Sect. 5).

The model treats the three methane isotopes as independent tracers, whose abundances are transformed non-linearly to and from the three more commonly used entities, total methane, $\delta^{13}C$ and $\Delta^{14}C$. The total methane is the sum of the three isotopes, though in practice, with abundances of ^{12}C, ^{13}C, ^{14}C approximately in the ratio $0.99{:}0.01{:}10^{-12}$, $^{14}CH_4$ can be excluded from the sum. Aside from this exclusion, the transformations are applied without approximation. Definitions of $\delta^{13}C$ and $\Delta^{14}C$ follow.

Following Craig (1953):

$$\delta^{13}C = R/R_{std} - 1 \tag{3}$$

where R is the isotopic molar ratio $^{13}C/^{12}C$ in the methane sample, and R_{std} is the corresponding ratio in the stable carbon isotope standard Vienna Peedee belemnite (VPDB) with accepted value 0.0112372 (Craig, 1957). While the usual "per mil" notation, ‰, is used to express both $\delta^{13}C$ and $\Delta^{14}C$ numerically, the multiplier 1000 is omitted from algebraic expressions such as Eq. (3). We refer to a methane sample as being isotopically "lighter" or "heavier" than another when its $\delta^{13}C$ value is lower or higher (ie, when it is less or more enriched in $^{13}CH_4$).

The definition of $\Delta^{14}C$ is more esoteric:

$$\Delta^{14}C = (A_{SN}/A_{abs}) - 1 \tag{4a}$$

The notation is that of Stuiver and Polach (1977, Table 1) except that we use the more usual $\Delta^{14}C$ in place of Δ, and λ_R in place of λ for the ^{14}C radioactive decay rate $(8267\,yr)^{-1}$. In Eq. (4a), A_{abs} is the "absolute international standard activity" defined for 1950 AD in the standard known as "0.95 NBS oxalic acid", and A_{SN} is the "normalized" sample activity (assumed to be corrected for "shelf" decay between sample

ACPD
6, 4995–5038, 2006

collection and ^{14}C analysis) expressed in term of the measured activity A_S through

$$A_{SN} = A_S \left(\frac{0.975}{1 + \delta^{13}C} \right)^2 \quad (4b)$$

Activities A_{abs}, A_{SN}, A_S are expressed in Bq per gram of carbon (Bq gC^{-1}), with A_{abs} having the accepted value 0.2260±0.0012 Bq gC^{-1} (Stuiver, 1980). The unit Bq (Becquerel, or disintegrations per second) equates to 433.2×10^{-15} mole(^{14}C).

The normalization in Eq. (4b) adjusts A_S to what it would have been had the sample had a $\delta^{13}C$ value of –25‰, the value for standard pre-industrial wood. This adjustment is based upon "mass-dependent isotope fractionation" in which isotope-specific chemical reaction rates, k_n, are inter-related through (e.g. Mook and van der Plicht, 1999)

$$k_{14}/k_{12} = (k_{13}/k_{12})^2 \quad (5)$$

Normalization (4b) ensures that the product carbon of a reaction bears the same $\Delta^{14}C$ value as the reactant carbon. The isotope-specific sink strengths $\lambda_n(t)$ would also satisfy Eq. (5), with the result that the sink evolution of $^{14}CH_4$ is fully specified in terms of those of $^{12}CH_4$ and $^{13}CH_4$:

$$\lambda_{14}(t) = \alpha\lambda_{13}(t) = \alpha^2\lambda_{12}(t) \quad (6)$$

with α the "isotope fractionation factor".

Some researchers report "percent modern carbon", pMC, in place of $\Delta^{14}C$ (e.g. Wahlen et al., 1989; Manning et al., 1990; Quay et al., 1999; Nakagawa et al., 2002), a usage borrowed from radiocarbon dating and without literal meaning in geochemical application, particularly for values exceeding 100% modern carbon in the nuclear era. The two are related through pMC=1+$\Delta^{14}C$, aside from implicit multipliers of 100 and 1000.

3 Source construction and mass-balancing sink

A history of methane sources from 1700 can be constructed by combining published inventories of natural sources (e.g. Lelieveld et al., 1998; Houweling et al., 2000) with "bottom-up" compilations of anthropogenic sources (e.g. Stern and Kaufmann, 1996; van Aardenne et al., 2001). All such constructions are subject to considerable uncertainty. We adopt three alternative anthropogenic source constructions as discussed below, each augmented by a common time-invariant natural inventory, taken to be that of Houweling et al. (2000) and totalling 222 Tg/yr (Table 1). While there may have been some changes to natural emissions over recent centuries (e.g. changes to wetland emissions due to climatic changes and/or to wetland management or drainage), such changes are likely to be smaller than emission uncertainty and much smaller than emission growth from human activities (Houweling et al., 2000). A very recent discovery of a previously unknown methane source from vegetation (Keppler et al., 2006) has implications for the pre-industrial and contemporary budgets that are neither understood nor tightly quantified. Thus, while we discuss the implications of this source, we do not include it in our source constructions.

The few available constructions of the anthropogenic source history are confined to the past ~100–150 years. We adopt the proxy-based construction of Stern and Kaufmann (1996, see also http://cdiac.ornl.gov/trends/meth/ch4.htm) for 1860–1994 (hereafter abbreviated "S&K"), and two versions of the EDGAR-HYDE inventory (http://mnp.nl/edgar/). The EDGAR-HYDE datasets (hereafter "E-H") are available as two alternate time series: (1) version 1.3 ("E-H v1.3") based on EDGAR 2.0 and described by van Aardenne et al. (2001) provides emission inventories every ten years over the period 1890–1990; and (2) version 1.4 ("E-H v1.4"), adjusted to match EDGAR 3.2 (Olivier and Berdowski, 2001; Olivier, 2002) provides inventories every ten years over 1890–1970 then every year to 1995.

We refer to each of three anthropogenic source histories, augmented by a fixed natural source inventory, annualized, and extrapolated back to 1700, as a "global source

inventory history" (GSIH) and shown in Fig. 1a from 1880.

In developing a plausible extrapolation of each GSIH back to 1700, we note the evidence by several researchers that an anthropogenic influence on methane emissions commenced well before the industrial era (e.g. Kammen and Marino, 1993; Subak, 1994; Houweling et al., 2000; Ruddiman and Thomson, 2001; Ferretti et al., 2005). Houweling et al. (2000) assessed the pre-industrial anthropogenic source at 30 Tg yr^{-1}, a value which we here associate with ca 1700. A linear interpolation between 30 Tg yr^{-1} in 1700 and the commencement of each source construction (1860 or 1890) preserves the proportional composition of the latter so that each anthropogenic inventory in 1700 differs slightly from that of Table 1. While linear interpolation is clearly an idealization in the absence of guiding data, it should assure that the disequilibrium in $\delta^{13}C$ propagates more realistically than spinning up from an initial state postulated for 1860 or 1890.

In summary, we employ three constructed GSIHs based on S&K, E-H v1.3 and E-H v1.4 (Fig. 1a). The source strength increases from 252 Tg yr^{-1} in 1700 to either 593 Tg yr^{-1} in 1994 (S&K), 542 Tg yr^{-1} in 1990 (E-H v1.3) or 524 Tg yr^{-1} in 1995 (E-H v1.4). It is clear (Fig. 1a) that both E-H GSIHs are weaker than S&K, especially since ca 1960, and weaker also than the contemporary source strength of ~600 Tg yr^{-1} that is needed to close the 'top-down' budget (Prather et al., 2001).

From the source and atmospheric histories of total methane the sink history required by mass balance, $\lambda(t)$, can be derived by solving Eq. (2) numerically at each time step. The result is shown in Fig. 1b in the form of turnover time $\tau(t)=\lambda(t)^{-1}$. The sinks matching the three GSIHs all display a weakening trend through the 20th century, qualitatively supporting the assessment of Lelieveld et al. (1998) and others of a slowed methane removal rate through the industrial era. In the 1980s all three sinks strengthen, qualitatively in line with chemistry-model calculations by Karlsdóttir and Isaksen (2000) and by Dentener et al. (2003). (The latter calculations appear to apply only the OH sink of methane so that while the lifetime against OH differs in definition from turnover time τ, that difference is manifested mainly as an offset leaving the trends directly comparable.)

The apparent increase in inter-annual variability in modelled sink strength from the late 1980s may be an artefact of the Etheridge-extended atmospheric dataset. The data to ca 1985 are smoothed, both naturally during air enclosure and statistically (Etheridge et al., 1998), whereas the more recent data exhibit the inter-annual variability captured in the NOAA/CMDL dataset.

4 Mass balance of $^{13}CH_4$ and the atmospheric history of $\delta^{13}C$

Two approaches are possible for modelling the evolution of $^{13}CH_4$. Both employ the mass-balancing sink history (Fig. 1b) from which separate sinks for $^{12}CH_4$ and $^{13}CH_4$ follow once an isotopic fractionation is specified (Sect. 4.1). In the first approach (Sect. 4.2), source histories for $^{12}CH_4$ and $^{13}CH_4$ are constructed and the respective atmospheric histories are deduced by forward modelling. The second approach (Sect. 4.3) exploits the detailed $\delta^{13}C$ time series now obtainable from air archived in polar ice and firn, enabling the $\delta^{13}C$ history in the global source to be inferred through inverse modelling of $^{13}CH_4$.

4.1 The evolving $^{13}CH_4$ sink

With the usual assumption that λ_{12} and λ_{13} are related through a fixed isotope fractionation factor $\alpha=\lambda_{13}(t)/\lambda_{12}(t)$, it is straightforward to deduce $\lambda_{12}(t)$ and $\lambda_{13}(t)$ separately from the inferred sink history $\lambda(t)$ in each time step by imposing mass balance for total methane and for each methane isotope. (Note our convention that α is defined with the minor isotope in the numerator, consistently with definition (3) for $\delta^{13}C$). Formally

$$\lambda_{13} = \alpha\lambda_{12} = \frac{1+W}{1+\alpha W}\alpha\lambda \qquad (7a)$$

ACPD
6, 4995–5038, 2006

in which W is the tropospheric mass ratio, $^{13}CH_4$:$^{12}CH_4$, given by

$$W = \frac{17}{16} R_{std}(1 + \delta) \quad (7b)$$

where δ denotes the tropospheric $\delta^{13}C$ value for that time step.

For multiple first-order methane sinks, α is the sink-weighted fractionation factor. Reported values for the dominant OH sink are α_{OH}=0.9946±0.0009 (Cantrell et al., 1990) and α_{OH}=0.9961±0.0004 (Saueressig et al., 2001); both of these are laboratory-based determinations and the cited uncertainties are 95% confidence intervals. The departure of α from unity is referred to as the kinetic isotope effect or KIE. It is useful to use ε=α−1, expressed in ‰, to quantify the KIE, so that ε_{OH} values that correspond to the above measured values for α_{OH} are –5.4‰ and –3.9‰, respectively. Separate KIEs apply to each removal process: for the soil sink ε_{soil} is near –20‰ (Tyler et al., 1994a; Snover and Quay, 2000), while for a minor active-chlorine sink $\varepsilon_{chlorine}$ is near –60‰ (Saueressig et al., 1995; Crowley et al., 1999; Tyler et al., 2000).

The large range of individual KIE values and uncertain relative sink strengths confer appreciable uncertainty on the sink-weighted mean KIE value, ε. Table 2 derives a plausible value for ε of –6.1±1.2‰ (95% confidence interval). Although the chlorine sink is of minor and uncertain magnitude, it discriminates strongly between isotopes and can therefore exert large "isotope leverage" on ε. As a result, the chlorine sink has been invoked to explain the $\delta^{13}C$ seasonal amplitude inferred from Southern Hemisphere observations (Allan et al., 2001; Platt et al., 2004), and a varying chlorine sink to explain inter-annual variability in those amplitudes (Allan et al., 2005).

Our approach is to select a value for ε for each GSIH that optimizes the fit to available data and, through comparison with the range –6.1±1.2‰, draw inferences about that GSIH.

ACPD
6, 4995–5038, 2006

4.2 Forward modelled $^{13}CH_4$

To each inventory component in each GSIH a representative $\delta^{13}C$ signature is assigned (Table 1). The weighted sum provides a $\delta^{13}C$ history, denoted $\delta_S(t)$, as companion to each GSIH, enabling separate $^{12}CH_4$ and $^{13}CH_4$ source histories to be derived. Individual $\delta^{13}C$ assignments have uncertainties that can exceed ~1‰ because of geographic variation and sparsity of measurement (e.g. Hein et al., 1997, Table 8; Quay et al., 1999, Table 1), so that $\delta_S(t)$ would have an uncertainty of similar magnitude.

From the constructed $^{12}CH_4$ and $^{13}CH_4$ source histories and the corresponding sink histories (with ε specified), the tropospheric $^{12}CH_4$ and $^{13}CH_4$ burdens are deduced by forward modelling (Eq. 2). These can be combined into $C(t)$ and the $\delta^{13}C$ evolutions, the latter denoted $\delta_A(t)$. The former, re-expressed as a mixing ratio, recovers the Etheridge-extended dataset. To first order $\delta_A(t)$ is given by $\delta_S(t)$–ε + disequilibrium correction (Lassey et al., 2000), so that varying ε essentially translates the $\delta_A(t)$ pattern parallel to the ‰-axis, and for each GSIH a value for ε can be chosen visually to optimize the fit of $\delta_A(t)$ to 20th century data (Fig. 2a).

It is clear that for the E-H sources in particular, the $\delta_A(t)$ pattern matches the observed pattern adequately for ca 1910–1990, even if the optimized ε has greater magnitude than expected to which we return below. For S&K the pattern and fractionation fits are less acceptable, displaying in particular a rate of change of $\delta_A(t)$ that is systematically too small for ca 1930–1950 then too great for ca 1950–1970. The poor fits before ca 1910 may be simply due to the less realistic source constructions in the prior decades in combination with the slow responsiveness of $\delta^{13}C$ to source changes (Tans, 1997; Lassey et al., 2000).

All data reported in Fig. 2a are from Southern Hemisphere (SH) sites. In particular, the post-1990 data rely heavily on the NIWA record for Baring Head (BHD), New Zealand, which is matched also by that for Scott Base, Antarctica (Lowe et al., 2004). The BHD record is based on high frequency sampling (~20 yr^{-1}) at a recognized clean-

ACPD
6, 4995–5038, 2006

EGU

air station, with data filtered for wind speed and direction. Clean-air records of comparable frequency are unavailable for the Northern Hemisphere (NH) during the 1990s. The BHD record features an "anomaly" in ca 1992 in which δ^{13}C falls markedly by ~0.2‰, followed by a slow recovery that a decade later has still not attained pre-1992 levels. This anomaly has been subjected to scrutiny (Lowe et al., 1997; Mak et al., 2000), and while it remains ill-explained, trans-equatorial transects (Mak et al., 2000) and NH observational records (Quay et al., 1999) suggest that it was largely confined to the extra-tropical SH, where available records cannot establish its longitudinal extent.

The values for ε that optimize the fit between simulated $\delta_A(t)$ and observational records are generally greater in magnitude than expected (Table 2) by at least 1‰. Potential explanations for this discrepancy include: (a) one or more δ^{13}C assignments for major inventory components are too light; (b) some GSIHs may have unrealistic source mixes, especially the mix of biogenic, fossil, and pyrogenic methane, and none include the newly-discovered terrestrial-plant source (Keppler et al., 2006); (c) methane in the SH troposphere is systematically lighter than the global mean; and/or (d) the estimate of the sink-weighted ε in Table 2 may be in error such as through underestimating the strength of the chlorine sink or an erroneous ε_{OH}. We now consider these four possibilities in turn.

Only for a major source such as global wetlands (assigned δ^{13}C value –60‰) can a reassignment of δ^{13}C materially affect the weighted mean $\delta_S(t)$ and thence ε. However, even the wetland source accounts for less than one third of the contemporary source, and so an assignment heavier by more than 3‰ (viz, δ^{13}C<–57‰) would be needed to raise $\delta_S(t)$ by ~1‰. Mikaloff Fletcher et al. (2004) assign a value -58‰ to the global wetland source which if adopted here would raise $\delta_S(t)$ by ~0.6‰. Uncertainties in individual source assignments can therefore account for uncertainty in inferred ε at least of order 1‰.

A global source with a greater proportion of pyrogenic and/or fossil methane (ie, relatively less biogenic methane) will be isotopically heavier, and would therefore require a ε value of smaller magnitude. Pyrogenic methane in particular exerts appreciable

isotopic leverage on $\delta^{13}C$ in the global source, especially from C_4 vegetation as fuel (Chanton et al., 2000). Moreover, assessments of the quantity of biomass fuel and its C_3:C_4 mix are highly uncertain (Kasischke and Penner, 2004; Mouillot et al., 2006), and the proportion of carbon emitted as methane is highly variable (Andreae and Merlet, 2001), with the result that the global pyrogenic methane source and its mean $\delta^{13}C$ signature are poorly determined. In addition, some fossil methane emissions such as from abandoned coal mines (e.g. Kirchgessner et al., 2000), or from natural gas seepages (Lacroix, 1993; Etiope and Klusman, 2002; Etiope, 2004) are poorly quantified and may be under-represented in the GSIH's used here. Moreover, larger pyrogenic and/or fossil components will not only make the source isotopically heavier, but the stronger source will better match independent top-down assessments (Prather et al., 2001).

Inclusion into the source inventory of the newly-discovered plant source (Keppler et al., 2006) would strengthen the global source. However, with a $\delta^{13}C$ value close to that of the mean source (averaging –50‰, according to Keppler et al. (2006), but dependent on the emission mix from C_3 and C_4 vegetation) that inclusion would have insufficient leverage to dramatically influence $\delta^{13}C$ in the global source. If however that source were included at the partial expense of biogenic methane from wetlands or rice cultivation to avoid possible double-counting of methane from these ecosystems, then the global source could be heavier and therefore require a mass-balancing fractionation of smaller magnitude. For example, including 80 Tg yr^{-1} of plant methane with signature –50‰ at the expense of 40 Tg yr^{-1} of biogenic methane (–60‰) would result in a global source that was both 40 Tg yr^{-1} stronger and ~1‰ heavier.

As noted, all observational data reported in Fig. 2a are from the SH, and are compared with simulated global means. It is well established that annual-mean SH methane is isotopically heavier than its NH counterpart by ~0.3‰ (Lowe et al., 1999; Quay et al., 1999; Miller et al., 2002). Such a mean N-S gradient is expected because with ~75% of sources in the NH (Fung et al., 1991) and $^{12}CH_4$ being removed faster than $^{13}CH_4$, methane in the SH has been airborne longer, is less abundant, and thence

is isotopically heavier than its NH counterpart. Thus, global-mean $\delta^{13}C$ histories might be expected to be ∼0.15‰ lighter than the SH datasets in Fig. 2a, which will reduce the optimizing choice of $|\varepsilon|$ by this amount.

The strength and geographic extent of the highly-fractionating chlorine sink is ill-determined (Platt et al., 2004). Based on the seasonalities in both mixing ratio and $\delta^{13}C$ for the SW Pacific marine boundary layer near New Zealand, Allan et al. (2005) deduce a "seasonal KIE" in the aggregate sink that varies between ∼–15‰ in 1994–1996 and ∼–7‰ in 1998–2000. These values cannot be accounted for by OH alone, and Allan et al. (2005) hypothesize that a chlorine sink operates in that marine boundary layer. While Allan et al. characterize the sink's likely seasonal amplitude and its variability in the SW Pacific, their analysis cannot shed light on the annual mean chlorine sink strength that might be folded into the sink-weighted ε of Table 2. More recent research suggests global methane removal by chlorine of ∼25 Tg yr^{-1} (W. Allan, personal communication, 2006) which if used in Table 2 would imply a sink-weighted fractionation of –7.5‰. The match with Table 2 would then be exemplary.

Determinations of ε_{OH} are inevitably laboratory based (Cantrell et al., 1990; Sauer-essig et al., 2001) and therefore open to question about transferability to the real-world atmosphere. Specifically, in the laboratory setting OH is artificially generated to artificially high OH density (∼10^{10} cm^{-3}) over a limited range of reactant temperatures with a possibly significant co-generation of other oxidants (e.g., $O(^1D)$). Furthermore, those two most recent determinations differ significantly (–5.4±0.9‰ and –3.9±0.4‰, respectively, with 95% confidence intervals). Thus the possibility that neither correctly reflect ε_{OH} in the real atmosphere cannot be dismissed.

4.3 Inverse modelled $^{13}CH_4$

A growing body of methane isotope data from air extracted from polar ice and firn allows an alternative approach to the evolving isotope balance. Sowers et al. (2005) and Ferretti et al. (2005) have reported data from Antarctic sites for air ages spanning the

past two centuries and the past two millennia, respectively. The post-1880 datasets are reported in Fig. 2a. From these datasets can be derived a smoothed annualized time series for atmospheric $\delta^{13}C$ that enable the $^{12}CH_4$ and $^{13}CH_4$ budgets to be closed by inverse modelling, yielding the corresponding sources, S_{12} and S_{13}.

An atmospheric $\delta^{13}C$ time series is generated by applying a smoothed fit to the combination of the Ferretti et al. (2005) dataset (to 1976) and contemporary high-frequency Baring Head dataset (annual means, 1988–2003) (updated from Lowe et al., 2004), with guidance from analyses of air archived from Cape Grim during 1978–1994 (Francey et al., 1999). The smoothing algorithm distinguishes variations in $\delta^{13}C$ that are not statistically proven from those that are well supported. It specifically weakens the "anomaly" from 1988–1994 in recognition of its possibly limited geographical extent. We refer to the annualized time series, 1700–2003, as the Ferretti-extended dataset, which in combination with the Etheridge-extended dataset enables separate $C_{12}(t)$ and $C_{13}(t)$ histories to be derived. In conjunction with the corresponding sink histories $\lambda_{12}(t)$ and $\lambda_{13}(t)$ of Eq. (7) that are based on ε values optimized from forward modelling (Fig. 2a), inverse modelling yields source histories $S_{12}(t)$ and$S_{13}(t)$ (by solving Eq. 2 for S_{12} and S_{13} in each time step). Their sum recovers the supplied methane source history $S(t)$ and their ratio provides companion $\delta^{13}C$ history, $\delta_S^{inv}(t)$. Figure 2b reports $\delta_S^{inv}(t)$ for S&K and E-H v1.4; that for E-H v1.3 (defined only to 1990) has a similar pattern to E-H v1.4.

Given that the forward modelled $\delta_A(t)$ fits the data quite well over ca 1910–1988, it is not surprising that inverse-modelled $\delta_S^{inv}(t)$ employing the same ε provides a smoothed match to the corresponding $\delta_S(t)$ over the same time interval. The departure of $\delta_S^{inv}(t)$ from $\delta_S(t)$ after ca 1988 is a direct reflection of the poor match between $\delta_A(t)$ for E-H v1.4 and the BHD post-anomaly observations, leading to a pronounced swing in $\delta_S^{inv}(t)$ towards a lighter source in the early 1990s that would be required to account for the smoothed 1990s data. Such a swing would have to be viewed as tentative at least until atmospheric $\delta^{13}C$ values are better characterized globally, and the inferred variations

ACPD
6, 4995–5038, 2006

in sink strength confirmed (Fig. 1b).

5 The radiomethane budget

Simulating the atmospheric history of radiomethane follows by applying budget closure to a construction of the radiomethane source history and the fractionation-adjusted sink history (Eq. 6). The simulated atmospheric $\Delta^{14}C$ evolution for each GSIH, denoted $\Delta_A(t)$, can then be constructed (Eq. 4), and is necessarily independent of α. The major challenge is in constructing the $^{14}CH_4$ source history, addressed in Sect. 5.1. Section 5.2 compares the construction with available $\Delta^{14}C$ source data, followed by an examination of $\Delta_A(t)$ and its implications in Sect. 5.3.

5.1 Constructing the radiomethane source

The generation, emission and atmospheric oxidation of methane is a pathway of the global carbon cycle. Radiomethane is an intrinsic participant in that pathway, and is present in all methane sources whose carbon has been derived from atmospheric CO_2 within the last few tens of millennia (^{14}C mean life is 8267 yr). Fossil methane sources are thus devoid of measurable radiomethane. For both biogenic and pyrogenic sources the radiomethane has cycled through the biosphere and accordingly we refer to it collectively as "biosphere-sourced radiomethane" (BSR).

Radiomethane is additionally produced during routine nuclear power generation, and vented to the atmosphere (e.g. Kunz, 1985; Povinec et al., 1986; Veres et al., 1995). We refer to this source as "nuclear power radiomethane" (NPR), and return to it below.

Recall that carbon-isotope fractionation during biochemical reactions, $CO_2 \rightarrow$ biosphere and biosphere $\rightarrow CH_4$ conserves $\Delta^{14}C$ values by virtue of the fractionation adjustment of Eq. (4b). The actual $\Delta^{14}C$ value in a biogenic or pyrogenic methane emission then depends only upon (a) the $\Delta^{14}C$ value in atmospheric CO_2 at photosynthesis of the included carbon, and (b) the time lapse between the carbon being fixed by

ACPD
6, 4995–5038, 2006

photosynthesis and being released in the form of methane. We refer to the time lapse as the "biospheric lag time" and denote it t_{lag}.

One would expect a wide rage of t_{lag} values, from less than a year (e.g. cattle consuming fresh grass that is quickly fermented in the rumen, grasslands burned at the end of the growing season) to many decades or longer (e.g. peat methanogenesis, burned forests), so that each methane-producing ecosystem and management regime would have a characteristic distribution of lag times. Note that t_{lag} values associated with the plant methane source (Keppler et al., 2006), were it to be included, cannot be estimated for lack of a known production mechanism. With a dearth of data from which to construct a lag-time distribution for any one ecosystem, we postulate a single distribution for the combined biospheric methane source. Specifically, we apply an exponential distribution of lag times with probability density function given by:

$$F(t_{lag}) = \tau_{lag}^{-1} \exp(-t_{lag}/\tau_{lag}) \quad (8)$$

in which τ_{lag} is the mean (and standard deviation) lag time in this one-parameter distribution. This need not imply that lag times for any one biogenic or pyrogenic inventory component be distributed according to function (8). The lag-time distribution is discussed further in Sect. 5.2.

Also required for constructing the BSR history is a history of $\Delta^{14}C$ in atmospheric carbon dioxide, denoted $\Delta_{CO2}(t)$. Although global coverage of $\Delta_{CO2}(t)$ measurements is poor, time series are available in both hemispheres (e.g. Manning et al., 1990; Levin and Kromer, 1997, 2004) and these can be extended using proxy measurements such as of tree rings (Stuiver and Quay, 1981; Hua and Barbetti, 2004). This enables a globally-representative time series for $\Delta_{CO2}(t)$ to be constructed, and we adopt that of Hua and Barbetti (2004), 1955–2000, merged with a pre-1955 series based on the tree-ring record of Stuiver and Quay (1981) (Fig. 3). The distinctive "pulse" commencing in ca 1954 is due to ^{14}C production initiated by nuclear weapon detonations in the atmosphere prior to the Limited Test Ban Treaty of 1963 (Nydal and Lövseth, 1983). The "bomb ^{14}C" quickly oxidized to ^{14}CO, then to $^{14}CO_2$, and thereafter participated

ACPD
6, 4995–5038, 2006

in the carbon cycle. Atmospheric $^{14}CO_2$ levels diminished steadily after peaking in 1964–1965 as the radiocarbon transferred to other carbon pools via photosynthesis and ocean dissolution, including indirectly to the atmospheric radiomethane pool.

The $\Delta^{14}C$ history in biospheric methane sources, denoted $\Delta_{BSR}(t)$, is a convolution of $\Delta_{CO2}(t)$, the lag distribution (8) and radioactive decay. For a particular GSIH the BSR source history (expressed in such units as mole($^{14}CH_4$) yr^{-1}) follows by combining $\Delta_{BSR}(t)$ with the strength and $\delta^{13}C$ of the non-fossil components of the GSIH. To this BSR source is added the NPR source whose construction is now described.

NPR is generated principally via the $^{14}N(n, p)^{14}C$ reaction on nitrogen dissolved in the reactor's water coolant and via $^{17}O(n, \alpha)^{14}C$ on oxygen in the oxide fuel and coolant. In the absence of sufficient data on emissions from nuclear facilities to fully characterize the NPR source strength and evolution, the standard approach has been to argue that PWRs (pressurized water reactors) are the predominant NPR source, and that the source strength is proportional either to the electrical power generated by PWR facilities or to the installed generating capacity as measures of the size of the PWR industry. We express the constant of proportionality in GBq($^{14}CH_4$) per GW_e-yr of generated electricity, and refer to it as the "NPR factor". That PWRs predominate as a source of NPR is due to the use of hydrogen as a cover gas in PWRs that results in most of the ^{14}C being vented as reduced species, $^{14}CH_4$, $^{14}C_2H_6$, etc rather than as $^{14}CO_2$ (Wahlen et al., 1989). Some ^{14}C may be retained in the fuel cladding and released during subsequent fuel reprocessing (Kunz, 1985; Povinec et al., 1986).

Based on measurements at or near individual PWR facilities, estimates of the NPR factor can be summarized as follows. (i) Detailed measurements at two US reactor sites (Kunz, 1985) yielded NPR factors 298 and 179 GBq($^{14}CH_4$) per GW_e-yr generated. These values are based on the total gaseous ^{14}C effluent reported by Kunz, the proportion of ^{14}C as hydrocarbon (90% and 74% at the two sites), and the $^{14}CH_4$ content of the hydrocarbon (77% and 68%). (ii) Based on routine monitoring of emissions from a Soviet-designed four-reactor facility in Hungary, 1988–1993, Veres et al. (1995) estimate hydrocarbon emissions ($^{14}C_nH_m$) at 740 GBq/GW_e-yr, which accounted for 94%

ACPD
6, 4995–5038, 2006

EGU

of ^{14}C emissions. That emissions are much higher than those from western-designed PWRs may be due to the use of nitrogen solutes as chemical regulators in the primary coolant (Veres et al., 1995). If we assume that 73% of the hydrocarbons were $^{14}CH_4$ based on Kunz (1985), the NPR factor would be 540 GBq($^{14}CH_4$) per GW_e-yr generated. (iii) Based on measurements from a 200 m tower in The Netherlands combined with trajectories and transport modelling, Eisma et al. (1995) infer $^{14}CH_4$ emission of 260±50 GBq per year per GW_e installed in NW Europe, which with a European-average load factor of 72% implies a mean NPR factor of 361±69 GBq($^{14}CH_4$) per GW_e-yr generated.

The 3-fold range of measurement-based NPR factors reported above may reflect design, engineering and operational differences among facilities, differing management regimes, different effluent-sampling strategies, uncertain electricity production data and load factors used, the varying proportions of $^{14}CH_4$ in the ^{14}C effluent (which is the usual measurement subject), and the extrapolation to annual emissions and electrical generation. Even the universal proportionality of methane release and electricity production is poorly founded.

Noting the above uncertainties, we have elected to treat the global-mean NPR factor as a parameter to be fitted empirically. An annual time series of global PWR-generated electrical energy is compiled to 2001 from IAEA data sourced and supplied by C. Tuniz (personal communication, 2002) (Table 3). While the time series prior to 1970 is less complete through applying a representative load factor, this has minimal practical impact here as PWR-generated electrical output grew 60-fold between 1970 and 1990.

5.2 Comparisons with source $\Delta^{14}C$ measurements

Simulations of $\Delta_{BSR}(t)$ (Fig. 3) are dependent upon the assumed distribution (8) of lag times. An exponential distribution is selected for its simplicity in the absence of guiding data, having just one selectable parameter to which the sensitivity of results can be tested. A disadvantage of such simplicity is that its mean and standard deviation cannot

be varied independently (they are numerically equal). Nevertheless, the application of such a continuous distribution should be more realistic than discrete distributions, such as the single lag time of 1 yr for all sources by Manning et al. (1990) and of 45 yr for wetland emissions by Quay et al. (1991), or the 2-component "rapid" and "aged" fractions considered by Wahlen et al. (1989).

It is instructive to compare $\Delta_{BSR}(t)$ simulations with measured $\Delta^{14}C$ in methane sources. Measurements have been made in methane sourced from wetlands, rice paddies, ruminant livestock, termites, and from biomass burning (Table 4). For more detail, see Wahlen et al. (1989) or summaries by Quay et al. (1991) or Nakagawa et al. (2002).

Measurements by Wahlen et al. (1989) cover a variety of sources, all measured during 1986–1988, and all in North America. During those years $\Delta_{CO2}(t)$ declined from 190‰ to 170‰ (global average, Fig. 3), which compares well with direct measurements of 190‰ that Wahlen et al. (1989) report. Consequently, a methane source with $\Delta^{14}C$ exceeding ~190‰ in 1986–1988 must have been mainly photosynthesised since ca 1958 (when $\Delta_{CO2}(t)$ rose through 190‰), suggesting mean biospheric lag times of up to ~30 years, whereas sources with $\Delta^{14}C$ significantly less than 170‰ must have been largely photosynthesised prior to ca 1958. Sources characterized by the lag distribution (8) with τ_{lag}≈6 years, a value that best fits available atmospheric data (Sect. 5.3), would have $\Delta^{14}C$≈250–280‰ when measured in 1986–1988 (Fig. 3); for smaller τ_{lag} the $\Delta^{14}C$ values would be lower. Consequently, the Wahlen et al. $\Delta^{14}C$ measurements for various biogenic sources in the range 100–260‰ are generally consistent with τ_{lag}≤6 years and/or τ_{lag}>30 years.

While the source measurements reported in Table 4 for ca 1986–1988 are only partially compatible with lag distribution (8) and τ_{lag}≈6 years, those measurements are mainly from northern mid-latitudes (and largely in the Americas) and provide a very sparse coverage of global biogenic and pyrogenic emissions. We therefore apply distribution (8) as a characterization of the global biospheric source, recognizing that it

ACPD
6, 4995–5038, 2006

will poorly characterize some individual ecosystem emissions.

5.3 The atmospheric radiomethane history

With radiomethane source and sink histories constructed, its atmospheric history can be inferred through forward modelling (Eq. 2), and the corresponding atmospheric history of $\Delta^{14}C$, denoted $\Delta_A(t)$, then constructed. The result for E-H v1.4 is shown in Fig. 4a for the τ_{lag} values of Fig. 3. Also shown in Fig. 4a are various $\Delta^{14}C$ measurement records from firn-entrapped air and from the contemporary atmosphere. The latter record includes annually-binned data since 1986, two thirds from the Southern Hemisphere (mainly from BHD) though N-S gradients are not discernible (Quay et al., 1999). The earliest contemporary measurements are those of Libby in ca 1950 (cited by Ehhalt, 1973, Table 1), and a single measurement by Bainbridge et al. (1961) in air collected in Gary, Indiana in 1960 that may have been contaminated by urban sources of fossil methane.

It should be recognised that air samples extracted from polar firn and ice are associated with a specific depth, but with a range of air ages due to diffusion and bubble-enclosure processes (Trudinger et al., 2002). The assignment of a mean air age therefore confers some uncertainty. Detailed analysis of air properties as a function of time should therefore take place after transforming into a function of ice/firn depth. While analyses such as these of data in Fig. 4 will be reported elsewhere (Etheridge et al., manuscript in preparation), they suggest a best-fit value $\tau_{lag} \approx 6$ years. This value is largely determined by data from ca 1960 to mid 1970s, and particularly by one specific datum for ca 1972, during the rise of the bomb ^{14}C pulse in $\Delta_A(t)$, which is particularly sensitive to τ_{lag} (Fig. 4a).

The NPR factor incorporated in Fig. 4a is 225 GBq/GW$_e$-yr, a value visually selected to best match available contemporary atmospheric data for $\tau_{lag} \approx 6$ years when using E-H v1.4. That selection is insensitive to τ_{lag} in the range 4–10 years, but for larger τ_{lag} a larger NPR factor would be appropriate. The selected NPR factor is also within the range determined through direct measurement at individual nuclear facilities

ACPD
6, 4995–5038, 2006

(Sect. 5.1).

With these optimized parameters for E-H v1.4 (τ_{lag}=6 yr, NPR factor = 225 GBq/GW$_e$-yr), the simulated NPR source comprises 32% of the total radiomethane source (BSR + NPR) of 48.4 mole yr^{-1} in 2000.

Figure 4b contrasts simulations with the E-H and S&K GSIHs both with τ_{lag}=6 yr, and also reports the fossil fractions for those GSIHs. While all three GSIHs can adequately account for available radiomethane data, S&K requires a NPR factor that is about 20% smaller, largely a result of the systematically smaller fossil fraction in S&K in recent decades. Conversely, for a GSIH with a larger fossil fraction a larger NPR factor would be inferred.

From Fig. 4 it is clear that determinants of $\Delta_A(t)$ fall into four distinct eras: (1) prior to ca 1960 it is anti-correlated with the fossil fraction, with inter-annual variations smoothed out by lag effects; (2) between ca 1960 and 1975 the rate of rise of $\Delta_A(t)$ is essentially determined by τ_{lag}; (3) between ca 1975 and 1990 τ_{lag} and the NPR source are both influential; (4) after ca 1990, provided that τ_{lag} is less than ~15 years, the NPR source is the dominant determinant of the rate of growth in $\Delta_A(t)$ while the fossil fraction influences both the absolute level and the optimized NPR factor. It will also be recalled that all ice and firn data have smoothed air ages due to processes of air enclosure (Trudinger et al., 2002). There are several corollaries to these observations.

First, Δ^{14}C measurements in the pre-nuclear era can yield estimates for the then-prevailing fossil fraction. However, for such measurements in the nuclear era, particularly post-1960, reliable fossil-fraction estimates are more problematic because of the confounding roles of both the propagating bomb ^{14}C pulse and the poorly quantified NPR source. Several investigators have estimated the fossil fraction from Δ^{14}C measurements in the 1980s and 1990s (Lowe et al., 1988; Wahlen et al., 1989; Manning et al., 1990; Quay et al., 1991, 1999), albeit with broad uncertainties arising from those confounding roles. A key finding of those investigations that is incorporated into IPCC emission inventories (Prather et al., 2001) is that fossil methane sources comprise about 20% of the contemporary global source (18±9% in the early 1990s, according to

Quay et al. (1999), in which the uncertainty appears to be dominated by a 30% uncertainty assigned to the strength of the NPR source). We return below to the potential for recalculating the fossil fraction.

A second corollary is that the rate of rise of $\Delta_A(t)$ during ca 1960–1975 could provide the best information on the global distribution of biospheric lag times. Previous assumptions about lag times are as diverse as 1 yr postulated by Manning et al. (1990) to 45 yr estimated for wetlands by Quay et al. (1991). This work applies a distribution of biospheric lag times with mean of 6 years, although a single datum for ca 1972 is pivotal to this estimate. More data for 1960–1975 would help elucidate the lag time distribution or permit separate distributions for different source categories. For example, applying a 2-parameter empirical distribution (e.g., log-normal) would enable constraints on τ_{lag} values to be segregated into separate constraints on the mean and standard deviation of that distribution. Alternatively, separate distributions could be applied to different sources categories.

A third corollary is that $\Delta^{14}C(CH_4)$ measurements in the post-1990 atmosphere could provide the best estimate of the global-mean NPR factor, though this factor is also influenced by both the prevailing fossil fraction and the τ_{lag} value if it exceeds ~15 years. This work favours a NPR factor of about 225 GBq (97 millimole) $^{14}CH_4$ per GW_e-yr of electricity generation by commercial PWRs, as long as fossil fraction is around 21–23% as embodied in the E-H GSIHs. For a fossil fraction near 17%, as per S&K, the fitted NPR factor is about 20% smaller. These estimates of NPR factor are compatible with the broad range inferred from measurements near individual PWR facilities, though may be too small to account for the rate of growth of atmospheric $\Delta^{14}C$ (Fig. 4).

The first and third corollaries suggest that ongoing atmospheric time series in $\Delta^{14}C(CH_4)$ would enable both the fossil fraction and the NPR factor to be given more certainty through concurrent estimation. This suggestion is addressed in a companion paper (Lassey et al., 2006).

ACPD
6, 4995–5038, 2006

6 Discussion and conclusions

This paper presents a comprehensive analysis of the evolution of the methane budget through the 20th century, using model simulations to examine the evolving carbon-isotope composition. The intent is to establish what information about that evolution can be gleaned from isotope measurements made in both contemporary air and air trapped in polar firn and ice. Studies of atmospheric methane from ice-entrapped air are now conveying information on past source inventories through isotope analysis made possible by new developments in mass spectrometry and in polar air extraction (Trudinger et al., 2002; Ferretti et al., 2005; Sowers et al., 2005). However, the air-sample size required for $^{14}CH_4$ analyses is still precluding detailed $^{14}CH_4$ information over century time scales.

Global source inventory histories such as the EDGAR-HYDE compilations (Olivier and Berdowski, 2001; van Aardenne et al., 2001; Olivier, 2002) constructed from economic, industrial and agricultural indicators are generally compatible with current knowledge on how the methane budget has evolved. However, the global E-H source, especially E-H v1.4, is weaker than IPCC assessments would suggest (Prather et al., 2001). By extending that knowledge to include $\delta^{13}C$ measurements the compatibility of the source mix with atmospheric $\delta^{13}C$ can be examined. In the present work we have shown that the global E-H source inventory for the 20th century is indeed generally compatible with newly-emergent $\delta^{13}C$ data from air trapped in Antarctic ice (Ferretti et al., 2005), with one a notable caveat. The isotopic fractionation, ε, in the global sink required to achieve compatibility (–6.7‰ and –7.2‰ for v1.3 and v1.4, respectively, when SH datasets of Fig. 2a are adjusted by ~0.2‰ to a global mean) is larger in magnitude than commonly accepted for the OH sink either alone or in tandem with a soil sink. However, such fractionation is within the range reported by Allan et al. (2005) to account for the seasonal amplitudes and their variation observed for the SW Pacific region. Allan et al. concur with the conclusion by Platt et al. (2004) that the highly-fractionating active-chlorine sink plays a significant role in the marine boundary

ACPD
6, 4995–5038, 2006

EGU

layer. The present analysis lends support to the role of chlorine, which is included in the indicative sink estimate of Table 2 and without which the ε values cited above would have even greater magnitude.

Alternatively or additionally, a heavier source would require less sink fractionation. This could be achieved with larger fossil and/or pyrogenic components, consistently with arguments that natural gas seeps are appreciably under-estimated (e.g. Etiope, 2004) and that carbon emissions from biomass combustion may be under-estimated (e.g. Mouillot et al., 2006). However, a revision of the fossil methane source would have to be compatible with estimates of the global fossil fraction based on $\Delta^{14}C(CH_4)$ data. Inclusion of the recently-discovered plant source (Keppler et al., 2006) in tandem with a reduction in the strength of the wetland and rice sources to avoid double-counting emissions from such ecosystems could both strengthen the global source and make it isotopically heavier, thereby reducing the sink fractionation required to balance the budget.

The more empirically based S&K source construction (Stern and Kaufmann, 1996), while stronger than the E-H sources, generally provides an inferior fit to 20th century $\delta^{13}C$ data (Fig. 2a).

In extending to the $^{14}CH_4$ (radiomethane) cycle, simulations based on the E-H source are broadly consistent with the sparse data available, but are not strongly challenged by those data. This analysis exposes the limitations on using radiomethane data to tightly constrain the fossil fraction in the methane source after ca 1960 AD, supporting the broad uncertainty associated with attempts to do so (e.g. Quay et al., 1999). The difficulty arises because the fossil fraction is only one determinant of atmospheric methane levels in the nuclear era. Another determinant is carbon dynamics through the biosphere, from photosynthetic uptake to methane emission via biogenesis or pyrogenesis, which control the biospheric propagation of the bomb ^{14}C pulse. A third determinant is the poorly-quantified nucleogenic production and release of radiomethane from nuclear power facilities. Nevertheless, radiomethane data from the pre-1960 atmosphere could constrain of fossil-fraction estimates from prior anthropogenic activities

and from natural geologic sources.

While the last two determinants confound fossil-fraction estimation during the nuclear era, they nevertheless provide opportunities. Radiomethane measurements in the atmosphere of 1960–1975 can potentially quantify carbon residence times in the biosphere between photosynthesis and methanogenesis ("biospheric lag times"), while similar measurements for the 1990s could elucidate both the strength of the nuclear-power source ("NPR factor") and the fossil fraction. The former suggests a mean biospheric lag time of 6 years. The latter is addressed in a companion paper (Lassey et al., 2006). As more and higher-resolution radiomethane measurements are made in air extracted from polar ice and firn, the roles of these determinants will be further clarified.

Acknowledgements. We are grateful to E. Dlugokencky (NOAA/ESRL, formerly NOAA/CMDL, Boulder, CO, USA) for supplying methane mixing ratio data prior to publication, and to S. Tyler (University of California, Irvine, CA, USA) and M. Wahlen (Scripps Institution of Oceanography, La Jolla, CA, USA) for supplying unpublished $\Delta^{14}C$ data for atmospheric methane. C. Tuniz (Australian Nuclear Science and Technology Organisation) kindly assembled and supplied data on electricity generation by the nuclear industry while seconded to Australian Permanent Mission to UN organisations and to IAEA in particular. The reporting of ^{14}C data has been clarified through discussions between one of us (A. M. Smith) and Q. Hua at ANSTO, Australia. A. Gomez (NIWA, New Zealand) compiled quality-controlled datasets from Baring Head, and provided a smoothed interpolation of atmospheric $\delta^{13}C$ data. Staff from the following institutes supported the Antarctic field work and ice archival: the Australian Antarctic Program; the Australian Bureau of Meteorology; CSIRO Marine and Atmospheric Research. This work was supported by the New Zealand Foundation for Research, Science and Technology under contract C01X0204, and by US National Science Foundation under grant OPP0087357.

References

Allan, W., Lowe, D. C., and Cainey, J. M.: Active chlorine in the remote marine boundary layer: Modeling anomalous measurements of $\delta^{13}C$ in methane, Geophys. Res. Lett., 28, 3239–

3242, 2001.
Allan, W., Lowe, D. C., Gomez, A. J., Struthers, H., and Brailsford, G. W.: Interannual variation of ^{13}C in tropospheric methane: Implications for a possible atomic chlorine sink in the marine boundary layer, J. Geophys. Res., 110, D11306, doi:10.1029/2004JD005650, 2005.
Andreae, M. O. and Merlet, P.: Emission of trace gases and aerosols from biomass burning, Global Biogeochem. Cycles, 15, 955–966, 2001.
Bainbridge, A. E., Suess, H. E., and Friedman, I.: Isotopic composition of atmospheric hydrogen and methane, Nature, 192, 648–649, 1961.
Bellisario, L. M., Bubier, J. L., Moore, T. R., and Chanton, J. P.: Controls on CH_4 emissions from a northern peatland, Global Biogeochem. Cycles, 13, 81–91, 1999.
Cantrell, C. A., Shetter, R. E., McDaniel, A. H., Calvert, J. G., Davidson, J. A., Lowe, D. C., Tyler, S. C., Cicerone, R. J., and Greenberg, J. P.: Carbon kinetic isotope effect in the oxidation of methane by the hydroxyl radical, J. Geophys. Res., 95, 22 455–22 462, 1990.
Chanton, J. P., Rutkowski, C. M., Schwartz, C. C., Ward, D. E., and Boring, L.: Factors influencing the stable carbon isotopic signature of methane from combustion and biomass burning, J. Geophys. Res., 105, 1867–1877, 2000.
Chanton, J. P., Bauer, J. E., Glaser, P. A., Siegel, D. I., Kelley, C. A., Tyler, S. C., Romanowicz, E. H., and Lazrus, A.: Radiocarbon evidence for the substrates supporting methane formation within northern Minnesota peatlands, Geochim. Cosmochim. Acta, 59, 3663–3668, 1995.
Craig, H.: The geochemistry of stable carbon isotopes, Geochim. Cosmochim. Acta, 3, 53–92, 1953.
Craig, H.: Isotopic standards for carbon and oxygen and correction factors for mass spectrometric analysis of carbon dioxide, Geochim. Cosmochim. Acta, 12, 133–149, 1957.
Craig, H., Chou, C. C., Welhan, J. A., Stevens, C. M., and Engelkemeir, A.: The isotopic composition of methane in polar ice cores, Science, 242, 1535–1539, 1988.
Crowley, J. N., Saueressig, G., Bergamaschi, P., Fischer, H., and Harris, G. W.: Carbon kinetic isotope effect in the reaction CH_4+Cl: a relative rate study using FTIR spectroscopy, Chem. Phys. Lett., 303, 268–274, 1999.
Cunnold, D. M., Steele, L. P., Fraser, P. J., Simmonds, P. G., Prinn, R. G., Weiss, R. F., Porter, L. W., O'Doherty, S., Langenfelds, R. L., Krummel, P. B., Wang, H. J., Emmons, L., Tie, X. X., and Dlugokencky, E. J.: In situ measurements of atmospheric methane at GAGE/AGAGE sites during 1985–2000 and resulting source inferences, J. Geophys. Res., 107, doi:10.1029/2001JD001226, 2002.

Dentener, F., Peters, W., Krol, M., van Weele, M., Bergamaschi, P., and Lelieveld, J.: Interannual variability and trend of CH_4 lifetime as a measure for OH changes in the 1979–1993 time period, J. Geophys. Res., 108, 4442, doi:10.1029/2002JD002916, 2003.
Dlugokencky, E. J., Masarie, K. A., Lang, P. M., and Tans, P. P.: Continuing decline in the growth rate of the atmospheric methane burden, Nature, 393, 447–450, 1998.
Dlugokencky, E. J., Houweling, S., Bruhwiler, L., Masarie, K. A., Lang, P. M., Miller, J. B., and Tans, P. P.: Atmospheric methane levels off: Temporary pause or a new steady–state?, Geophys. Res. Lett., 30, 1992, doi:10.1029/2003GL018126, 2003.
Dlugokencky, E. J., Myers, R. C., Lang, P. M., Masarie, K. A., Crotwell, A. M., Thoning, K. W., Hall, B. D., Elkins, J. W., and Steele, L. P.: Conversion of NOAA atmospheric dry air CH_4 mole fractions to a gravimetrically prepared standard scale, J. Geophys. Res., 110, D18306, doi:10.1029/2005JD006035, 2005.
Ehhalt, D. H.: Methane in the atmosphere. In: Carbon and the Biosphere, Proceedings of the 24th Brookhaven Symposium in Biology,, edited by: Woodwell, G. M. and Pecan, E. V., US Atomic Energy Commission, Springfield, VA, USA, 144–158, 1973.
Eisma, R., Vermeulen, A. T., and van der Borg, K.: $^{14}CH_4$ emissions from nuclear power plants in northwestern Europe, Radiocarbon, 37, 475–483, 1995.
Etheridge, D. M., Steele, L. P., Francey, R. J., and Langenfelds, R. L.: Atmospheric methane between 1000 A.D. and present: Evidence of anthropogenic emissions and climate variability, J. Geophys. Res., 103, 15 979–15 993, 1998.
Etheridge, D. M., Smith, A. M., Lowe, D. C., Trudinger, C. M., Langenfelds, R. L., Steele, L. P., Lassey, K. R., Levchenko, V. A., and Manning, M. R.: Sources of atmospheric methane during the 20th century from methane isotopic measurements in Antarctic firn air, in: 8^{th} Scientific Assembly of IAMAS, Innsbruck, Austria, pp. 106, 2001.
Etiope, G.: New directions: GEM – Geologic emissions of methane, the missing source in the atmospheric methane budget, Atmos. Environ., 38, 3099–3100, 2004.
Etiope, G. and Klusman, R. W.: Geologic emissions of methane to the atmosphere, Chemosphere, 49, 777–789, 2002.
Ferretti, D. F., Miller, J. B., White, J. W. C., Etheridge, D. M., Lassey, K. R., Lowe, D. C., MacFarling Meure, C. M., Dreier, M. F., Trudinger, C. M., van Ommen, T. D., and Langenfelds, R. L.: Unexpected changes to the global methane budget over the past 2000 years, Science, 309, 1714–1717, 2005.
Francey, R. J., Manning, M. R., Allison, C. E., Coram, S. A., Etheridge, D. M., Langenfelds, R.

L., Lowe, D. C., and Steele, L. P.: A history of $d^{13}C$ in atmospheric CH_4 from the Cape Grim Air Archive and Antarctic firn air, J. Geophys. Res., 104, 23 631–23 643, 1999.
Fung, I., John, J., Lerner, J., Matthews, E., Prather, M., Steele, L. P., and Fraser, P. J.: Three-dimensional model synthesis of the global methane cycle, J. Geophys. Res., 96, 13 033–13 065, 1991.
Hein, R., Crutzen, P. J., and Heimann, M.: An inverse modeling approach to investigate the global atmospheric methane cycle, Global Biogeochem. Cycles, 11, 43–76, 1997.
Houweling, S., Dentener, F., and Lelieveld, J.: Simulation of preindustrial methane to constrain the global source strength of natural wetlands, J. Geophys. Res., 105, 17 243–17 255, 2000.
Houweling, S., Kaminski, T., Dentener, F., Lelieveld, J., and Heimann, M.: Inverse modeling of methane sources and sinks using the adjoint of a global transport model, J. Geophys. Res., 104, 26 137–26 160, 1999.
Hua, Q. and Barbetti, M.: Review of tropospheric bomb ^{14}C data for carbon cycle modeling and age calibration studies, Radiocarbon, 46, 1273–1298, 2004.
Kammen, D. M. and Marino, B. D.: On the origin and magnitude of pre-industrial anthropogenic CO_2 and CH_4 emissions, Chemosphere, 26, 69–86, 1993.
Karlsdóttir, S. and Isaksen, I. S. A.: Changing methane lifetime: Possible cause for reduced growth, Geophys. Res. Lett., 27, 93–96, 2000.
Kasischke, E. S. and Penner, J. E.: Improving global estimates of atmospheric emissions from biomass burning, J. Geophys. Res., 109, D14S01, doi:10.1029/2004JD004972, 2004.
Keppler, F., Hamilton, J. T. G., Braß, M., and Röckmann, T.: Methane emissions from terrestrial plants under aerobic conditions, Nature, 439, 187–191, 2006.
Kirchgessner, D. A., Piccot, S. D., and Masemore, S. S.: An improved inventory of methane emissions from coal mining in the United States, J. Air Waste Manage. Assoc., 50, 1904–1919, 2000.
Kunz, C.: Carbon-14 discharge at three light-water reactors, Health Phys., 49, 25–35, 1985.
Lacroix, A. V.: Unaccounted-for sources of fossil and isotopically-enriched methane and their contribution to the emissions inventory: A review and synthesis, Chemosphere, 26, 505–557, 1993.
Lassey, K. R., Lowe, D. C., and Manning, M. R.: The trend in atmospheric methane $d^{13}C$ and implications for isotopic constraints on the global methane budget, Global Biogeochem. Cycles, 14, 41–49, 2000.
Lassey, K. R., Lowe, D. C., and Smith, A. M.: The atmospheric cycling of radiomethane and the

"fossil fraction" of the methane source, Atmos. Chem. Phys. Discuss., 6, 5039–5056, 2006.
Lelieveld, J., Crutzen, P. J., and Dentener, F. J.: Changing concentration, lifetime and climate forcing of atmospheric methane, Tellus, 50B, 128–150, 1998.
Lelieveld, J., Peters, W., Dentener, F. J., and Krol, M. C.: Stability of tropospheric hydroxyl chemistry, J. Geophys. Res., 107, 4715, doi:10.1029/2002JD002272, 2002.
Levin, I. and Kromer, B.: Twenty years of high precision atmospheric $^{14}CO_2$ observations at Schauinsland station, Germany, Radiocarbon, 39, 205–218, 1997.
Levin, I. and Kromer, B.: The tropospheric $^{14}CO_2$ level in mid-latitudes of the Northern Hemisphere (1959–2003), Radiocarbon, 46, 1261–1272, 2004.
Lowe, D., Manning, M., Levin, I., Wahlen, M., Tyler, S., Etheridge, D., and Lassey, K.: Radiocarbon content of atmospheric methane and the 'fossil fraction' of emissions, in: 8th Scientific Assembly of IAMAS, Innsbruck, Austria, pp. 106, 2001.
Lowe, D. C., Brenninkmeijer, C. A. M., Tyler, S. C., and Dlugokencky, E. J.: Determination of the isotopic composition of atmospheric methane and its application in the Antarctic, J. Geophys. Res., 96, 15 445–15 467, 1991.
Lowe, D. C., Manning, M. R., Brailsford, G. W., and Bromley, A. M.: The 1991–1992 atmospheric methane anomaly: Southern Hemisphere ^{13}C decrease and growth rate fluctuations, Geophys. Res. Lett., 24, 857–860, 1997.
Lowe, D. C., Brenninkmeijer, C. A. M., Manning, M. R., Sparks, R. J., and Wallace, G.: Radiocarbon determination of atmospheric methane at Baring Head, New Zealand, Nature, 332, 522–525, 1988.
Lowe, D. C., Koshy, K., Bromley, T., Allan, W., Struthers, H., Mani, F., and Maata, M.: Seasonal cycles of mixing ratio and ^{13}C in atmospheric methane at Suva, Fiji, J. Geophys. Res., 109, D23308, doi:10.1029/2004JD005166, 2004.
Lowe, D. C., Allan, W., Manning, M. R., Bromley, A., Brailsford, G., Ferretti, D., Gomez, A., Knobben, R., Martin, R., Mei, Z., Moss, R., Koshy, K., and Maata, M.: Shipboard determinations of the distribution of ^{13}C in atmospheric methane in the Pacific, J. Geophys. Res., 104, 26 125–26 135, 1999.
Mak, J. E., Manning, M. R., and Lowe, D. C.: Aircraft observations of $\delta^{13}C$ of atmospheric methane over the Pacific in August 1991 and 1993: Evidence of an enrichment in $^{13}CH_4$ in the Southern Hemisphere, J. Geophys. Res., 105, 1329–1335, 2000.
Manning, M. R., Lowe, D. C., Moss, R. C., Bodeker, G. E., and Allan, W.: Short term variations

in the oxidizing power of the atmosphere, Nature, 436, 1001–1004, 2005.
Manning, M. R., Lowe, D. C., Melhuish, W. H., Sparks, R. J., Wallace, G., Brenninkmeijer, C. A. M., and McGill, R. C.: The use of radiocarbon measurements in atmospheric studies, Radiocarbon, 32, 37–58, 1990.
Martens, C. S., Kelley, C. A., Chanton, J. P., and Showers, W. J.: Carbon and hydrogen isotopic characterization of methane from wetlands and lakes of the Yukon-Kuskokwim Delta, Western Alaska, J. Geophys. Res., 97, 16 689–16 701, 1992.
Mikaloff Fletcher, S. E., Tans, P. P., Bruhwiler, L. M., Miller, J. B., and Heimann, M.: CH_4 sources estimated from atmospheric observations of CH_4 and its $^{13}C/^{12}C$ isotopic ratios: 2. Inverse modeling of CH_4 fluxes from geographical regions, Global Biogeochem. Cycles, 18, GB4005, doi:10.1029/2004GB002224, 2004.
Miller, J. B., Mack, K. A., Dissly, R., White, J. W. C., Dlugokencky, E. J., and Tans, P. P.: Development of analytical methods and measurements of $^{13}C/^{12}C$ in atmospheric CH_4 from NOAA Climate Monitoring and Diagnostics Laboratory Global Air Sampling Network, J. Geophys. Res., 107, doi:10.1029/2001JD000630, 2002.
Mook, W. G. and van der Plicht, J.: Reporting ^{14}C activities and concentrations, Radiocarbon, 41, 227–239, 1999.
Mouillot, F., Narasimha, A., Balkanski, Y., Lamarque, J.-F., and Field, C. B.: Global carbon emissions from biomass burning in the 20th century, Geophys. Res. Lett., 33, L01801, doi:10.1029/2005GL024707, 2006.
Nakagawa, F., Yoshida, N., Sugimoto, A., Wada, E., Yoshioka, T., Ueda, S., and Vijarnsorn, P.: Stable isotope and radiocarbon compositions of methane emitted from tropical rice paddies and swamps in Southern Thailand, Biogeochem., 61, 1–19, 2002.
Nydal, R. and Lövseth, K.: Tracing bomb ^{14}C in the atmosphere 1962–1980, J. Geophys. Res., 88, 3621–3642, 1983.
Olivier, J. G. J.: On the quality of global emission inventories, PhD thesis, Utrecht, Utrecht, Netherlands, 167 pp, 2002.
Olivier, J. G. J. and Berdowski, J. J. M.: Global emission sources and sinks, in: The Climate System, edited by: Berdowski, J., Guicherit, R., and Heij, B. J., A. A. Balkema Publishers/Swets & Zeitlinger Publishers, Lisse, The Netherlands, 33–78, 2001.
Platt, U., Allan, W., and Lowe, D.: Hemispheric average Cl atom concentration from $^{13}C/^{12}C$ ratios in atmospheric methane, Atmos. Chem. Phys., 4, 2393–2399, 2004.
Povinec, P., Chudý, M., and Sivo, A.: Anthropogenic radiocarbon: past, present, and future,

Radiocarbon, 28, 668–672, 1986.
Prather, M., Ehhalt, D., Dentener, F., Derwent, R., Dlugokencky, E., Holland, E., Isaksen, I., Katima, J., Kirchhoff, V., Matson, P., Midgley, P., and Wang, M.: Atmospheric chemistry and greenhouse gases, in: Climate Change 2001: The Scientific Basis, Contribution of Working Group I to the Third Assessment Report of the Intergovernmental Panel on Climate Change, edited by: Houghton, J. T., Ding, Y., Griggs, D. J., Nogeur, M., van der Linden, P. J., Dai, X., Maskell, K., and Johnson, C. A., Cambridge University Press, Cambridge, UK, 239–287, 2001.
Prinn, R. G., Huang, J., Weiss, R. F., Cunnold, D. M., Fraser, P. J., Simmonds, P. G., McCulloch, A., Harth, C., Reimann, S., Salameh, P., O'Doherty, S., Wang, R. H. J., Porter, L. W., Miller, B. R., and Krummel, P. B.: Evidence for variability of atmospheric hydroxyl radicals over the past quarter century, Geophys. Res. Lett., 32, L07809, doi:10.1029/2004GL022228, 2005.
Quay, P. D., Stutsman, J., Wilbur, D., Snover, A., Dlugokencky, E. J., and Brown, T.: The isotopic composition of atmospheric methane, Global Biogeochem. Cycles, 13, 445–461, 1999.
Quay, P. D., King, S. L., Stutsman, J., Wilbur, D. O., Steele, L. P., Fung, I., Gammon, R. H., Brown, T. A., Farwell, G. W., Grootes, P. M., and Schmidt, F. H.: Carbon isotopic composition of atmospheric CH_4: fossil and biomass burning source strengths, Global Biogeochem. Cycles, 5, 25–47, 1991.
Robbins, R. C., Cavanagh, L. A., Salas, L. J., and Robinson, E.: Analysis of ancient atmospheres, J. Geophys. Res., 78, 5341–5344, 1973.
Ruddiman, W. F. and Thomson, J. S.: The case for human causes of increased atmospheric CH_4 over the last 5000 years, Quaternary Science Reviews, 20, 1769–1777, 2001.
Saueressig, G., Bergamaschi, P., Crowley, J. N., Fischer, H., and Harris, G. W.: Carbon kinetic isotope effect in the reaction of CH_4 with Cl atoms, Geophys. Res. Lett., 22, 1225–1228, 1995.
Saueressig, G., Crowley, J. N., Bergamaschi, P., Brühl, C., Brenninkmeijer, C. A. M., and Fischer, H.: Carbon 13 and D kinetic isotope effects in the reaction of CH_4 with $O(^1D)$ and OH: New laboratory measurements and their implications for the isotopic composition of stratospheric methane, J. Geophys. Res., 106, 23 127–23 138, 2001.
Snover, A. K. and Quay, P. D.: Hydrogen and carbon kinetic effects during soil uptake of atmospheric methane, Global Biogeochem. Cycles, 14, 25–39, 2000.
Sowers, T., Bernard, S., Aballain, O., Chappellaz, J., Barnola, J.-M., and Marik, T.: Records of the $d^{13}C$ of atmospheric CH_4 over the last 2 centuries as recorded in Antarctic snow and ice,

Global Biogeochem. Cycles, 19, GB2002, doi:10.1029/2004GB002408, 2005.
Stern, D. I. and Kaufmann, R. K.: Estimates of global anthropogenic methane emissions 1860–1993, Chemosphere, 33, 159–176, 1996.
Stuiver, M.: Workshop on ^{14}C data reporting, Radiocarbon, 22, 964–966, 1980.
Stuiver, M. and Polach, H. A.: Reporting of ^{14}C data, Radiocarbon, 19, 355–363, 1977.
Stuiver, M. and Quay, P. D.: Atmospheric ^{14}C changes resulting from fossil fuel CO_2 release and cosmic ray flux variability, Earth Planet. Sci. Lett., 53, 349–362, 1981.
Subak, S.: Methane from the house of Tudor and the Ming Dynasty: Anthropogenic emissions in the sixteenth century, Chemosphere, 29, 843–854, 1994.
Tans, P. P.: A note on isotope ratios and the global atmospheric methane budget, Global Biogeochem. Cycles, 11, 77–81, 1997.
Trudinger, C. M., Etheridge, D. M., Rayner, P. J., Enting, I. G., Sturrock, G. A., and Langenfelds, R. L.: Reconstructing atmospheric histories from measurements of air composition in firn, J. Geophys. Res., 107, 4780, doi:10.1029/2002JD002545, 2002.
Tyler, S. C., Crill, P. M., and Brailsford, G. W.: $^{13}C/^{12}C$ fractionation of methane during oxidation in a temperate forested soil, Geochim. Cosmochim. Acta, 58, 1625–1633, 1994a.
Tyler, S. C., Brailsford, G. W., Yagi, K., Minami, K., and Cicerone, R. J.: Seasonal variations in methane flux and d$^{13}CH_4$ values for rice paddies in Japan and their implications, Global Biogeochem. Cycles, 8, 1–12, 1994b.
Tyler, S. C., Ajie, H. O., Rice, A. L., Cicerone, R. J., and Tuazon, E. C.: Experimentally determined kinetic isotope effects in the reaction of CH_4 with Cl: Implications for atmospheric CH_4, Geophys. Res. Lett., 27, 1715–1718, 2000.
van Aardenne, J. A., Dentener, F. J., Olivier, J. G. J., Klein Goldewijk, C. G. M., and Lelieveld, J.: A 1°×1° resolution data set of historical anthropogenic trace gas emissions for the period 1890–1990, Global Biogeochem. Cycles, 15, 909–928, 2001.
Veres, M., Hertelendi, E., Uchrin, G., Csaba, E., Barnabás, I., Ormai, P., Volent, G., and Futó, I.: Concentration of radiocarbon and its chemical forms in gaseous effluents, environmental air, nuclear waste and primary water of a pressurized water reactor power plant in Hungary, Radiocarbon, 37, 497–504, 1995.
Wahlen, M., Tanaka, N., Henry, R., Deck, B., Zeglen, J., Vogel, J. S., Southon, J., Shemesh, A., Fairbanks, R., and Broecker, W.: Carbon-14 in methane sources and in atmospheric methane: The contribution from fossil carbon, Science, 245, 286–290, 1989.
Wang, J. S., Logan, J. A., McElroy, M. B., Duncan, B. N., Megretskaia, I. A., and Yan-

tosca, R. M.: A 3-D model analysis of the slowdown and interannual variability in the methane growth rate from 1988 to 1997, Global Biogeochem. Cycles, 18, GB3011, doi:10.1029/2003GB002180, 2004.

Wang, Y. and Jacob, D. J.: Anthropogenic forcing on tropospheric ozone and OH since preindustrial times, J. Geophys. Res., 103, 31 123–31 135, 1998.

Table 1. An indicative inventory postulated for 1700 AD, and $\delta^{13}C$ assignments[a].

Source component	Strength Tg yr^{-1}	$\delta^{13}C$ ‰
Natural Sources		
Wetlands	163	–60
Termites	20	–57
Wildfires	5	–25
Oceans	15	–40
Wild animals	15	–62
Geologic	4	–40
Natural subtotal	222	–57.4
Anthropogenic Sources		
Coal mining	0	–35
Other fossil	0	–40
Farmed livestock	5	–62
Animal wastes	0	–55
Rice cultivation	10	–64
Forest burning, woodfuel	5	–25
Savanna burning	5	–12
Waste treatment, landfills	5	–55
Anthropogenic subtotal	30	–47.0
Total source	**252**	**–56.1**

[a] Source strengths and $\delta^{13}C$ assignments are taken from Houweling et al. (2000), except that anthropogenic biomass burning is split into forest and savanna biomass with $\delta^{13}C$ assignments typical of C_3 and C_4 vegetation (Chanton et al., 2000). The anthropogenic inventory is notional only, and the inventory used at 1700 AD is that for the earliest year specified by a particular source construction (1860 or 1890), scaled down to 30 Tg yr^{-1}.

ACPD
6, 4995–5038, 2006

Table 2. Typical construction of an aggregate sink[a].

Sink	Strength Tg yr^{-1}	ε_{sink} ‰
OH	490±85	−4.65±0.75
soil	30±15	−20±2
stratosphere	40±8	0±0[b]
chlorine	10±9	−60±1
Total	**570±87**	**−6.1±1.2**

[a] Removal rates and 95% confidence intervals in sinks other than chlorine are from the IPCC Second Assessment Report (Schimel et al., 1996); the Third Assessment Report (Prather et al., 2001) neither substantially updates these nor supplies uncertainty estimates. The chlorine sink is from Platt et al. (2004), with plausible confidence interval. The KIE values are literature based (see text) with ε_{OH} the mean of two published values (Cantrell et al., 1990; Saueressig et al., 2001). The confidence interval in the KIE value for individual sinks accounts for the spread in measured values. In calculating confidence intervals for the total sink and corresponding KIE, all individual confidence intervals are assumed to be uncorrelated.

[b] While processes that destroy stratospheric methane discriminate against $^{13}CH_4$, the return ^{13}C-enriched flux is minor and ignored in our model, consistently with IPCC assessments. Consequently the stratosphere is viewed as a transport-mediated sink that is isotopically neutral.

ACPD
6, 4995–5038, 2006

Table 3. Annual electrical power production by pressurized water reactors (PWRs)[a].

Year	Production GW(e).hr	Year	Production GW(e).hr
1960	652	1981	386 392
1961	652	1982	422 642
1962	1698	1983	484 765
1963	1698	1984	597 703
1964	2713	1985	707 940
1965	2713	1986	785 148
1966	2955	1987	854 791
1967	8053	1988	936 338
1968	9977	1989	1 015 396
1969	13 346	1990	1 060 232
1970	19 002	1991	1 115 182
1971	30 009	1992	1 157 002
1972	40 376	1993	1 179 096
1973	54 054	1994	1 226 937
1974	90 091	1995	1 254 243
1975	158 485	1996	1 306 979
1976	174 300	1997	1 270 385
1977	233 481	1998	1 328 329
1978	264 673	1999	1 361 315
1979	256 771	2000	1 386 121
1980	303 188	2001	1 113 419

[a] Dataset kindly supplied by C. Tuniz, Australian Permanent Mission to UN organizations, Vienna (personal communication, 2002), and sourced from IAEA. Production data 1960–1969 is unavailable, and the entries above for those years are installed capacities multiplied by the average load factor of 44.5% for 1970–1974.

ACPD
6, 4995–5038, 2006

Table 4. Measured $\Delta^{14}C$ values in methane sources.

Year(s)	Location	$\Delta^{14}C$, ‰	Reference
	Wetlands (various)		
1986–88	NY, USA (43° N)	110–197	Wahlen et al. (1989)
1987	MN, Canada (59° N)	108–155	Wahlen et al. (1989)
1986	WV, USA (39° N)	156–203	Wahlen et al. (1989)
c. 1987	AK, USA	110±40	Quay et al. (1991)
c. 1987	Amazon	200±40	Quay et al. (1991)
c. 1987	MN, USA	230±60	Quay et al. (1991)
1988	AK, USA (61° N)	−42 – 205	Martens et al. (1992)
1991	Thailand (6° N)	100±20	Nakagawa et al. (2002)
1991	MN, USA (47° N)	135–161	Chanton et al. (1995)
1993–94	MN, Canada (55° N)	148–275	Bellisario et al. (1999)
	Rice paddies		
1987	LA, USA (30° N)	104–181	Wahlen et al. (1989)
1990	Japan (36° N)	58–161	Tyler et al. (1994a)
1991	Japan (36° N)	127–155	Tyler et al. (1994a)
1991	Thailand (6° N)	270±10	Nakagawa et al. (2002)
	Ruminants		
1986–88	USA	176–210	Wahlen et al. (1989)
	Termites		
1987	USA	238±18	Wahlen et al. (1989)
	Biomass burning		
1987	USA	165–403	Wahlen et al. (1989)

ACPD
6, 4995–5038, 2006

EGU

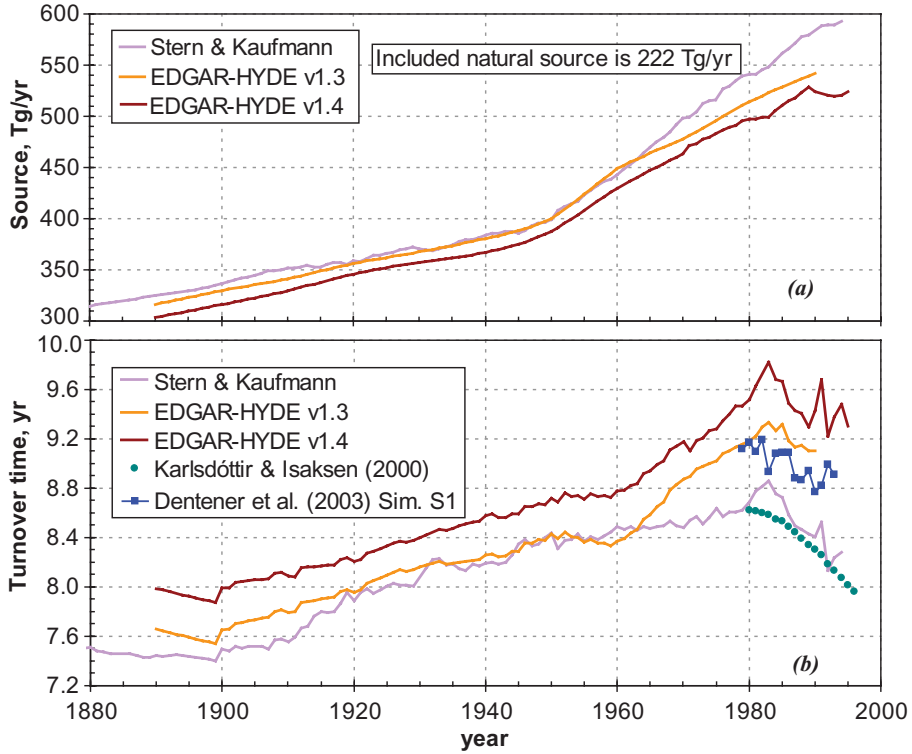

Fig. 1. **(a)** Three "bottom-up" constructions of the anthropogenic source history, each augmented by a natural source of 222 Tg yr^{-1}. Each construction, with its underlying inventory, is referred to as a "Global Source Inventory History" (GSIH). **(b)** The histories of methane turnover time, $\tau(t)=\lambda(t)^{-1}$ corresponding to the GSIHs and consistent with the Etheridge-extended atmospheric dataset. Also shown are model calculations by Karsldóttir and Isaksen (2000) and by Dentener et al. (2003, Simulation S1) of turnover times due to the OH sink alone for which trends, but not absolute values, can be compared with $\tau(t)$.

ACPD
6, 4995–5038, 2006

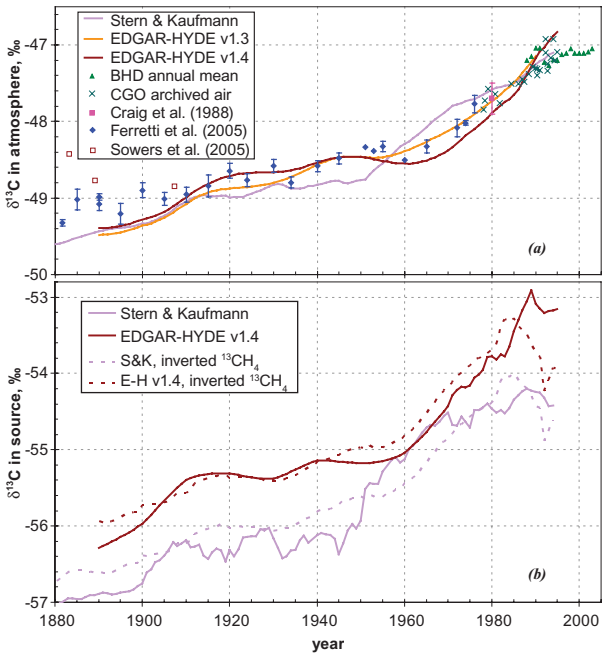

Fig. 2. (a) The modelled histories of $\delta^{13}C$ in atmospheric methane, $\delta_A(t)$, based on the three GSIHs of Fig. 1a combined with $\delta^{13}C$ assignments for individual sources (Table 1), and corresponding sink histories of Fig. 1b. Available data are also shown: air trapped in polar firn or ice as indicated; air archived at Cape Grim Observatory (Francey et al., 1999); contemporary time series of annual means from Baring Head (updated from Lowe et al., 2004). The KIE value, ε, is optimized separately for each source history at –8.1‰, –6.9‰ and –7.4‰ for S&K, E-H v1.3 and E-H v1.4 respectively. **(b)** The source history of $\delta^{13}C$, δ_S (t), used to generate panel (a) for S&K and for E-H v1.4 (solid lines), compared with the corresponding $\delta_S^{inv}(t)$ deduced by inverse modelling (dotted lines). The corresponding history for E-H v1.3 is little different from E-H v1.4 apart from an offset in the range 0.4–0.8‰.

ACPD
6, 4995–5038, 2006

EGU

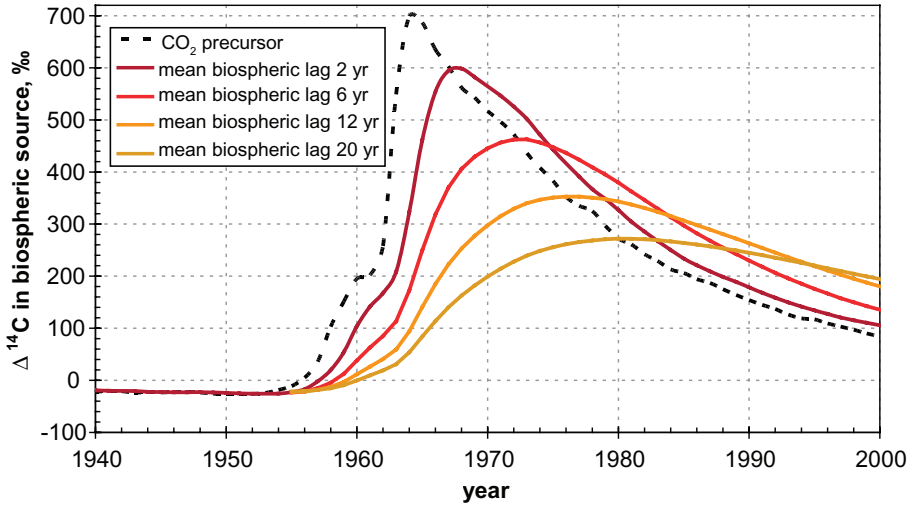

Fig. 3. The simulated history of $\Delta^{14}C$ in methane from biospheric sources, $\Delta_{BSR}(t)$, is shown for several mean biospheric lag times, τ_{lag}, of between 2 and 20 years. This construction depends only upon the $\Delta^{14}C$ history in precursor photosynthesised CO_2, $\Delta_{CO2}(t)$, which is also shown (Hua and Barbetti, 2004), and upon the distribution of biospheric lag times between photosynthesis and methanogenesis (Eq. 8).

ACPD
6, 4995–5038, 2006

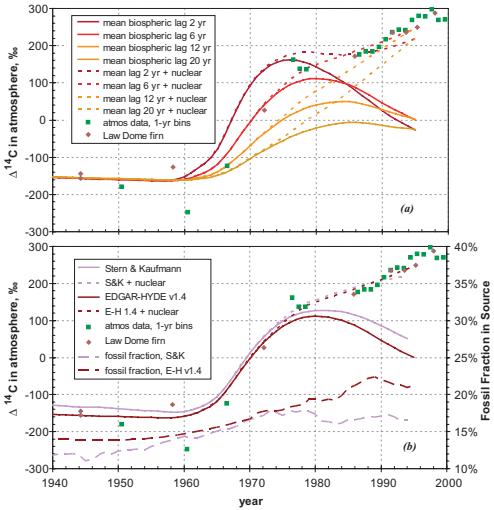

Fig. 4. A simulated $\Delta^{14}C$ history in atmospheric methane, $\Delta_A(t)$. Solid lines show the biosphere-sourced radiomethane (BSR) only, and the dashed lines show the augmentation from nuclear-power radiomethane (NPR) using a value for the NPR factor selected to optimise the fit to data for a mean biospheric lag time, τ_{lag}, of 6 years. Two observational records are reported. The first is a composite record of 239 data points in contemporary air from both hemispheres, collated by Lowe et al. (2001) into annual bins. That record includes unpublished data kindly contributed by S. Tyler, and M. Wahlen, as well as data from New Zealand. The second record is based on air trapped in Antarctic firn at Law Dome (Etheridge et al., unpublished data). For post-1986 measurements, including pre-1986 firn air, uncertainties are of order 10‰. Each firn-air datum additionally carries time uncertainty due to the distribution of air ages in each sample. **(a)** Simulations for E-H v1.4 for a range of τ_{lag} values. **(b)** Simulations for S&K and E-H v1.4 are contrasted (E-H v1.3 is little different from v1.4) for a common value for τ_{lag} of 6 years. Also shown in (b) is the "fossil fraction" in the two source constructions (long-dash lines, RH scale), which is the source fraction that is derived from ^{14}C-free carbon in geological deposits. The NPR factors used for E-H v1.4 and S&K are respectively 225 and 175 GBq/GW(e), selected to best fit contemporary data.

ACPD
6, 4995–5038, 2006